Research On Near Ground Precision Application Navigation Technology Of Plant Protection UAV Based On SRCKF-SLAM

Dandan Wang[1,2*], Zhaokun Zhu[3], Kaituo Tan[1], Hongjie Li[4], and Liang Yu[1]

[1] School of Mechanical and Electrical Engineering, Huainan normal university, Huainan Anhui,P.R.China, 232038
[2] Human-computer collaborative robot Joint Laboratory of Anhui Province, Huainan Anhui,P.R.China, 232038
[3] School of Information Engineering, Zhengzhou Technology and Business University, Zhengzhou Henan,P.R.China,475000
[4] College of Electronic Information and Electrical Engineering, Anyang Institute Of Technology, Anyang Henan, P.R. China,455000
[*] Corresponding author. E-mail: lansejingling1988@126.com

Received: Apr. 01, 2023; Accepted: Jun. 30, 2024

The traditional quaternion is used as the description parameter of the nonlinear state model of the aircraft, and the accuracy of the attitude estimation is presented. A square root cubature Kalman filter algorithm based on quaternion is proposed. The algorithm takes the attitude quaternion error and the gyro drift error as the state quantity, and measures the attitude quaternion of SINS/SLAM navigation. The square root cubature Kalman filter algorithm is used for pose estimation, which not only solves the standardization problem of traditional quaternion, but also reduces the state dimension and complexity of the square root UKF algorithm of traditional quaternion, and improves the numerical stability.

Keywords: modern precision agriculture; plant protection UAV; SRCKF-SLAM; attitude angle estimation

http://dx.doi.org/10.6180/jase.202506_28(6).0009

1. Introduction

In view of the serious liquid leakage and inaccurate operation of traditional spraying equipment in the process of application, the self-propelled spray bar spray machine can achieve accurate application in the field environment, but it is difficult for some plant protection machinery such as hills, paddy fields and mountains to enter the complex environment. As the intelligent assistant of China's "precision agriculture" - UAV, it plays a key role in the success of the "precision agriculture aviation protection", and the realization of an all-round, full coverage, no repeated application of precision medicine mission, depends on the UAV's aviation flight path planning and navigation positioning [1–3]. In terms of agricultural precision application [4, 5], the use of aerial UAV [6, 7] has greatly promoted the development of mechanized crop management. Among them, navigation technology is a core technology for service UAV, plant protection UAV and guidance UAV, and is the key to realize the intelligence and autonomy of UAV. At the same time, the development of navigation technology also promotes the rapid development of aerial plant protection UAV to a large extent, providing scientific basis and operational efficiency for the popularization of aerial precision operation of UAV.

In order to achieve efficient and accurate work of plant protection UAV, first of all, it depends on whether the UAV position can be accurately perceived, that is, whether the positioning accuracy of UAV navigation can ensure the production efficiency and operation accuracy of intelligent agriculture. The UAV carries a series of sensors to complete the accurate judgment of the operation path, the accurate identification of the operation ridge line [8], and the judgment of the crop growth status, and then carries out the next step of high-precision navigation aviation spraying, spraying management and other steps. With the development of automatic navigation technology of plant protection UAV [9], the requirements for its positioning accuracy

and stability are getting higher and higher.

The fusion of velocity information and position information, position information and attitude information, or velocity information and attitude information through sensors can obtain positioning with higher accuracy than a single sensor [10].

In view of the development status and future development trend of UAV navigation technology in recent years, it is found that visual navigation [11] is a research hotspot and trend of UAV because of its high level of intelligence and rich information through comparison of various navigation methods; In combination with the development field and characteristics of plant protection UAV, research on visual navigation in the mode of GPS, simultaneous localization and mapping, SLAM [12] and other auxiliary navigation to accurately locate the carrier and obtain accurate position information, and then obtain the optimal solution of UAV position estimation through data fusion technology [13, 14], so as to achieve real-time positioning and assist in completing the path planning of UAV, The position of UAV is observed and estimated to improve the navigation accuracy. The main algorithms for UAV navigation attitude estimation are EKF, UKF, CDKF, SRUKF, Bayes inference, SRCKF, etc. But their disadvantages are as follows :

1. Extended Kalman filter (EKF) [15] ignores Taylor's higher order part and introduces truncation error.

2. Unscented Kalman Filtering (UKF) algorithm [16] estimates the system state quantity and covariance by weighting based on the U transformation. However, due to the complexity of matrix decomposition and its inversion, it is difficult to guarantee the positive definite covariance.

3. Central Difference Kalman filter belongs to a suboptimal Gaussian filter. This algorithm uses polynomial interpolation method to calculate multi-dimensional integral. In form, the sampling point weight and the prediction covariance expression are different from UKF algorithm. Theoretically, CDKF and UKF algorithm [17, 18] have the same or slightly higher precision.

4. The standard CKF algorithm [19], due to the large amount of computation in the recursive process, leads to the numerical instability. The literature proposed the strong tracking filter (STF) volume Kalman filter algorithm, which introduced the fading factor to achieve the online adjustment of the gain matrix, thus maintaining the high tracking and positioning capability when the system dimension changes, but also increasing the computational complexity, which makes it difficult to ensure the numerical calculation and filtering accuracy.

Fig. 1. Environment

To solve the above problems, this paper continues to use the square root filter. By recursively updating in the square root form of the covariance matrix, it can not only reduce the computational complexity, but also ensure the symmetry and semi positive determination of the covariance matrix, improve the accuracy and stability of the filter. This algorithm is sufficient to meet the navigation and positioning accuracy of the plant protection UAV.

When the UAV is used to spray pesticides, the overall mass of the UAV will change with time, that is, variable load flight. At this time, it needs to use a more advanced control algorithm to control its flight attitude for simulation. SRCKF-SLAM algorithm is use.

Flight Dynamics of Plant Protection UAV: Motor voltage and torque equations for UAV.

$$\begin{cases} u_a = iR_a + L_a\frac{di}{dt} + k_e w \\ J_m\frac{dw}{dt} = M_m - M_{\text{load}} \end{cases} \tag{1}$$

Where, u_a is the Voltage of motor. i is the current of motor. R_a is the equivalent resistance, L_a is the inductance, w is the angular velocity of the rotor, k_e is the back electromotive force coefficient, J_m is the rotational inertia of the rotor, M_m is the torque of the rotor, and M_{load} is the load torque of the UAV during flight.

The motor used for UAVs is relatively small, so the inductance is also relatively small and can be ignored. Simplify Eq. (1):

$$i = \frac{u - k_e w}{R_a} \tag{2}$$

Rewrite the motor dynamics equation as:

$$J_m\frac{dw}{dt} = \frac{k_m u}{R_a} - \frac{k_e k_m w}{R_a} - M_{\text{load}} \tag{3}$$

In the formula, when the high-order infinitesimal quantity is ignored, $M_m = k_m i.M_{\text{load}}$ and w are intrinsically related, and the initial value is expanded by Taylor, so

$$w_m = -Aw + Bu + C \tag{4}$$

Where, A , B , and C are constants, ignoring constant C yields, so

$$\frac{w(s)}{u(s)} = \frac{B}{s + A} \tag{5}$$

Select a three-phase brushless DC motor. When the line is connected and the receiver receives control signals from the remote control, the motor will adjust its speed according to different commands to achieve the expected flight attitude of the UAV [20–22].

2. Materials and methods

This section may be divided by subheadings. It should provide a concise and precise description of the experimental results, their interpretation, as well as the experimental conclusions that can be drawn.

SLAM algorithm status parameter:

$$\begin{cases} x = \begin{bmatrix} x_v & x_m \end{bmatrix}^T \\ P = \begin{bmatrix} P_v & P_{vm} \\ P_{vm}^T & P_{mm} \end{bmatrix} \end{cases} \tag{6}$$

Where, x_v is the carrier state quantity; x_m is the characteristic state quantity of environmental road sign; P_w is the carrier covariance matrix; P_{vm} is the correlation covariance matrix between the carrier and the feature map; P_{mm} is the characteristic covariance matrix.

The SLAM problem is described as a posterior probability density model as:

$$p\left(x_k \mid u_k, z_k\right) = p\left(z_k \mid x_{v,k}, x_m\right) \times \int p\left(x_{v,k} \mid x_{v,k-1}, u_k\right) \cdot p\left(x_{v,k-1}, x_m \mid u_{k-1}, z_{k-1}\right) dx_{v,k-1} \tag{7}$$

Where, u_k is the control input; $p\left(x_{v,k} \mid x_{v,k-1}, u_k\right)$ is the motion model; $p\left(z_k \mid x_{v,k}, x_m\right)$ is the measurement model.

SLAM general nonlinear motion model is:

$$\begin{cases} x_k = f\left(x_{k-1}\right) + w_{k-1} \\ z_k = h\left(x_k\right) + v_k \end{cases} \tag{8}$$

Where, $f\left(x_{k-1}\right)$ and $h\left(x_k\right)$ are system nonlinear functions and observation functions respectively; Representation of $w_k \sim N(0, Q)$ system noise and $v_k \sim N(0, R)$ observation noise; x_k represents the carrier state at time k.

Cubature rules:

$$\begin{cases} I(f) = \int_{R^n} f(x) \exp\left(-x^T x\right) dx \\ I(f) \approx \sum_{i=1}^{2n} w_i f\left(\xi_i\right) \\ \xi_i = \sqrt{n}\{1\}_i, i = 1, 2, \cdots, 2n \\ w_i = 1/2n, i = 1, 2, \cdots, 2n \end{cases} \tag{9}$$

Where, n is the dimension of state quantity, and the total number of volume points is $2n.\xi_i$ is the coordinate of mutually orthogonal volume point set in the i dimensional coordinate system. Lete be the unit column vector, which $e = [1, 0, \cdots, 0]^T$. $\{1\}_i$ represents the i-th set of fully symmetric points that completely arrange element e and change element symbols.

When $n = 2$, the base of volume point under 2D coordinate system is $\sqrt{2}\left\{\begin{bmatrix} 1 \\ 0 \end{bmatrix}, \begin{bmatrix} 0 \\ 1 \end{bmatrix}, \begin{bmatrix} -1 \\ 0 \end{bmatrix}, \begin{bmatrix} 0 \\ -1 \end{bmatrix}\right\}$. (w_i, ξ_i) is the volume point set of $2n$ selected points with the same weight.

CKF algorithm principle

1. Time Update:

$$\begin{cases} P_{k-1|k-1} = S_{k-1|k-1} S_{k-1|k-1}^T \\ X_{i,k-1|k-1} = S_{k-1|k-1} \xi_i + \hat{x}_{k-1|k-1} \\ X_{i,k-1|k-1}^* = f\left(x_{i,k-1|k-1}\right) \\ \hat{x}_{k|k-1} = \frac{1}{m} \sum_{i=1}^{m} X_{i,k,k-1}^* \\ P_{k|k-1} = \frac{1}{m} \sum_{i=1}^{m} x_{i,k,k-1}^* x_{i,k,k-1}^* - \hat{x}_{k|k-1} \hat{x}_{k,k-1}^T + Q_{k-1} \end{cases} \tag{10}$$

Where, $p\left(x_{k-1}\right) = N\left(\hat{x}_{k-1|k-1}, P_{k-1|k-1}\right)$, which is the posterior probability density at $k-1$ time. m is the dimension of SLAM state quantity, and the joint volume rule is $2n$; $X_{i,k-1|k-1}^*$ is the volume point representing the state quantity at $k-1$ time; $\hat{x}_{k|k-1}$ is the predicted value of state quantity at time k; $P_{k|k-1}$ is the prediction value of state error covariance at time k.

2. Measurement update.

$$\begin{cases} P_{k-1|k-1} = S_{k-1|k-1} S_{k-1|k-1}^T \\ X_{i,k-1|k-1} = S_{k-1|k-1} \xi_i + \hat{x}_{k-1|k-1} \\ X_{i,k-1|k-1}^* = f\left(x_{i,k-1|k-1}\right) \\ \hat{x}_{k|k-1} = \frac{1}{m} \sum_{i=1}^{m} X_{i,k,k-1}^* \\ P_{k|k-1} = \frac{1}{m} \sum_{i=1}^{m} x_{i,k,k-1}^* x_{i,k,k-1}^* - \hat{x}_{k|k-1} \hat{x}_{k,k-1}^T + Q_{k-1} \end{cases} \tag{11}$$

Where, $z_{i,k|k-1}$ is the observed measurement of the i th volume point; $\hat{z}_{k|k-1}$ is the observation prediction value at time k.$P_{zz,k|k-1}$ is the autocorrelation covariance; $P_{xz,k|k-1}$ is the correlation covariance. W_k is the Kalman gain; $\hat{x}_{k|k}$ is the state estimation at time k; $P_{k|k}$ is the covariance of state error at time k.

CKF algorithm principle

1. Time update According to the state prediction value $\hat{x}_{k|k-1}$ at time k obtained in (2), calculate the prediction error covariance square root factor $S_{k|k-1}$ and state parameter.

$$\begin{cases} P_{k-1|k-1} = S_{k-1|k-1} S_{k-1|k-1}^T \\ X_{i,k-1|k-1} = S_{k-1|k-1} \xi_i + \hat{x}_{k-1|k-1} \\ X_{i,k-1|k-1}^* = f\left(x_{i,k-1|k-1}\right) \\ \hat{x}_{k|k-1} = \frac{1}{m} \sum_{i=1}^{m} X_{i,k,k-1}^* \\ P_{k|k-1} = \frac{1}{m} \sum_{i=1}^{m} x_{i,k,k-1}^* x_{i,k,k-1}^* - \hat{x}_{k|k-1} \hat{x}_{k,k-1}^T + Q_{k-1} \end{cases} \tag{12}$$

Where, $T(\cdot)$ is the sub formula for calculating the square root of the matrix; $S_{Q,k-1}$ is the square root of observation error Q_{k-1}.

2.1. Measurement update.

According to the algorithm, the predicted value of time observation is estimated.

$$\begin{cases} S_{zz,k|k-1} = T\left(\left[\varsigma_{k|k-1} \;\; S_{R,k}\right]\right) \\ R_k = S_{R,k} S_{R,k}^T \\ \varsigma_{k|k-1} = \frac{1}{m}\left[z_{1,k|k-1} - \hat{z}_{k|k-1} \;\; z_{2,k|k-1} - \hat{z}_{k|k-1} \cdots z_{m,k|k-1} - \hat{z}_{k|k-1}\right] \\ P_{xz,k|k-1} = \eta_{k|k-1} \varsigma_{k|k-1}^T \\ \eta_{k|k-1} = \frac{1}{\sqrt{m}}\left[x_{1,k|k-1} - \hat{x}_{k|k-1} \;\; x_{2,k|k-1} - \hat{x}_{k|k-1} \cdots x_{m,k|k-1} - \hat{x}_{k|k-1}\right] \\ W_k = \frac{\left(\frac{P_{xz,k|k-1}}{S_{zz,k|k-1}^T}\right)}{\left(\frac{P_{xz,k|k-1}}{S_{zz,k|k-1}}\right)} \\ S_{k|k} = T\left(\left[\eta_{k|k-1} - W_k \varsigma_{k|k-1} \;\; W_k S_{R,k}\right]\right) \end{cases} \tag{13}$$

Where, $S_{zz,k|k-1}$ is the square root factor of prediction error covariance; $S_{R,k}$ is the square root of the system random error R_k; $P_{xz,k|k-1}$ is the estimated cross correlation square root factor; $S_{k|k}$ is error covariance factor.

3. Experimental setup

3.1. Extraction of orchard environment

Using the unmanned aerial vehicle navigation path as shown in the Fig. 1 to implement pesticide spraying and other technologies on the sampling plot, and verifying the positioning accuracy of the warranty unmanned system under the following parameters.

The Kmeans clustering image processing method is used to obtain a segmented image, such as Fig. 2(1), which undergoes 100 iterations. K-means clustering algorithm is unsupervised learning and can segment the image into several parts. The method is to cluster or group data points with similar features together.

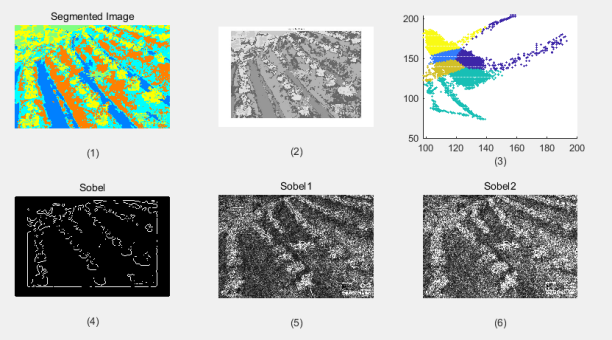

Fig. 2. Extraction of orchard environment

Fig. 2 (2) is obtained by applying grayscale processing to Fig. 2(1), with the aim of facilitating feature extraction and segmentation of the image. The characteristic of unsupervised learning is does not require the use of labeled data, and the algorithm will recognize patterns and similarities among multiple sets of data. So give k-means any unlabeled dataset, such as the pixel values of an image, and then let k-means decompose this dataset into k clusters, where k is a variable. It can be clearly seen from the Fig. 2(3) that the characteristics of crops are different from those of field ridges and surrounding weeds, which can effectively extract feature information of 5 different color classifications from the complex surrounding environment.

Because the sobel operator is a weighted average operator that utilizes fast convolution calculation, its weight is inversely proportional to the distance from adjacent points to the center point, and the gradient amplitude is consistent when detecting edges in different directions.Therefore, this article selects the sobel operator for image processing of orchard environments.

Fig. 2 (4) is obtained by using the Sobel operator to extract edges when no threshold is specified in Fig. 2 (1). In order to achieve adaptive edge detection effect, Fig. 2(5) and Fig. 2(6) are obtained by using the sum of gradient square roots and absolute values, respectively. It can be seen that the image edge segmentation effect obtained by using the self use threshold method is the best.

This article focuses on the backend image processing of images collected from UAV plant protection operations. The experiment is a simulation experiment and does not involve physical flight. The UAV state model parameters mentioned in the article are set parameters, and three filtering algorithms are simulated and analyzed under the given parameters.

Table 1. CKF algorithm execution steps

Start
Calculate the Cubature point sets ξ_i, and the parameter $X_{i,k\|k-1}$;
Navigation calculation of fruit location information.
Calculate the predicted value of the state variable $\hat{X}_{i,k\|k-1}$ and the predicted value of the square root of the error covariance $S_{k\|k-1}$
Propagating cubature points through observation equations and square roots of cross-correlation covariance matrix $P_{xz,k\|k-1}$
Calculate Kalman gain K_k
End

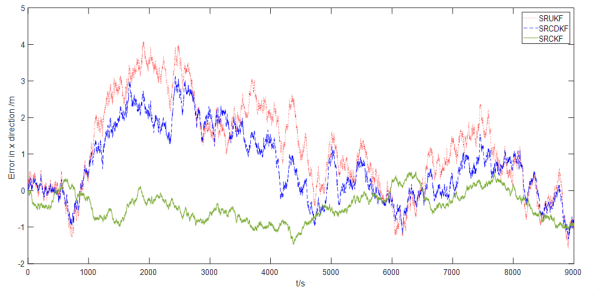

Fig. 3. Error in x direction

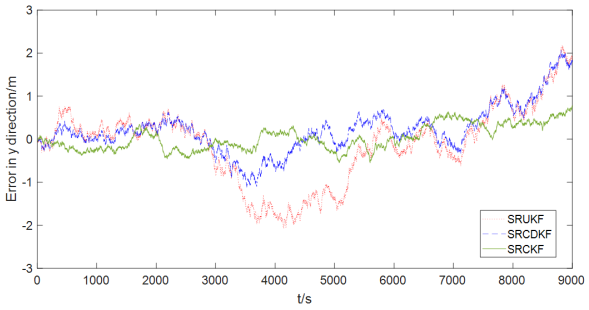

Fig. 4. Error in y direction

3.2. Simulation and Analysis of Aircraft Attitude Estimation Based on SRCKF Algorithm

Assume that the initial state of the carrier is zero, the sampling frequency of the sensor $T = 0.02$ s, and the system noise and observation noise are $Q = \begin{bmatrix} 0.25^2 & 0 & 0 \\ 0 & 0.03^2 & 0 \\ 0 & 0 & 0.2^2 \end{bmatrix}$ and $R = \begin{bmatrix} 0.1^2 & 0 & 0 \\ 0 & 0.01^2 & 0 \\ 0 & 0 & 0.1^2 \end{bmatrix}$ respectively. The motion parameters of the carrier are as follows: velocity $v = 1$ m/s, velocity error $\sigma_v = 0.1$ m/s, maximum angular velocity $\alpha = 3°/s$. Under the above experimental environment, 50 independent repeated simulation experiments were conducted based on SRCKF-SLAM, SRUKF-SLAM and SCDKF-SLAM, and the estimation errors in the x direction and y direction of the carrier path were analyzed and compared.

It can be seen from the figure that the maximum estimation error of the SRUKF algorithm is about 4 m , and the maximum estimation error of the SRCDKF algorithm is about 3 m , and the estimation error of the two algorithms gradually decreases to about 1 m after 4500 s of simulation time; However, as the simulation time goes on, the filtering error of the two algorithms increases gradually due to the large amount of numerical calculation caused by the large number of state quantity dimensions of the two algorithms. In a word, the estimation error of the two algorithms fluctuates greatly and the filtering is unstable during the whole simulation time; Based on the SRCKF algorithm, the estimation error of the x-direction of the carrier position is basically between $[-1, 1]$m. The stability is better than SRUKF and SRCDKF algorithms, and the error fluctuation is small.

It is assumed that the plant protection UAV travels along a straight line, and the flight direction is set to the y direction of the coordinate system. Therefore, the estimation errors of the three filtering algorithms in this direction are correspondingly reduced compared with the estimation errors of the x direction. It can be seen from the figure that the error range of the SRUKF algorithm based tracking estimation of the carrier position in the y direction is about $[-2, 2]$m, and the SRCDKF algorithm based estimation error range is $[-1, 2]$m. The estimation error range based on SRCKF algorithm is $[-0.5, 0.8]$m, which is more stable than SRUKF and SRCDKF algorithms.

As can be seen from the figure, the error fluctuation trend of SRUKF and SRCDKF algorithms for tracking and estimating the carrier position in the z direction is basically the same, and the maximum error is about 2.2 m . The convergence speed of the two algorithms is basically the same, which is consistent with the computational complexity of the two algorithms. The algorithm based on SRCKF estimated the carrier position in the z direction. In the 2000s

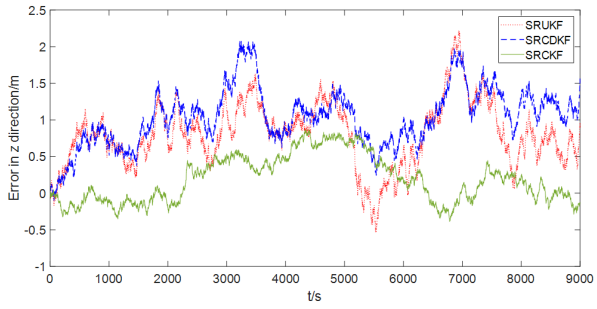

Fig. 5. Error in z direction

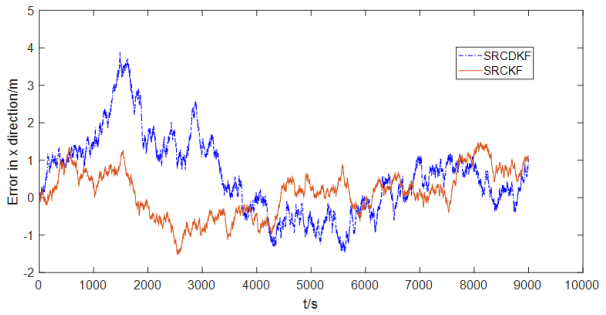

Fig. 6. Error in x direction

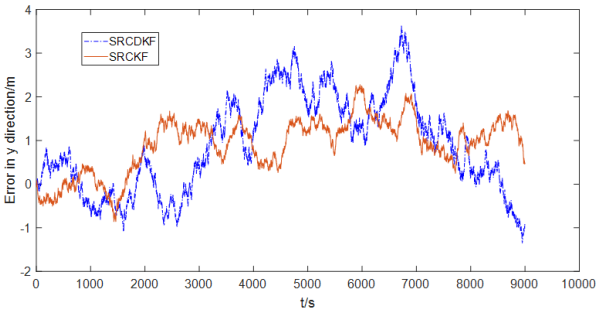

Fig. 7. Error in y direction

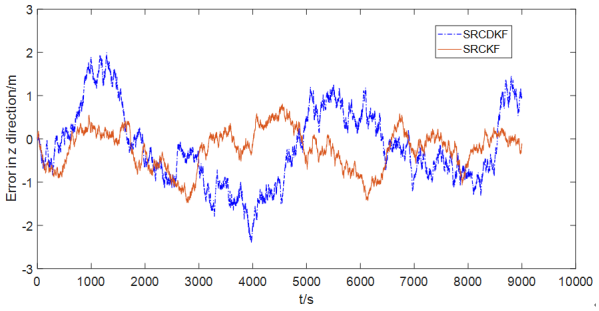

Fig. 8. Error in z direction

before the simulation time, the error was basically small; in addition, with the continuous increase of the volume points and the constant update of the state parameters, the error increased slightly, but within 0.8 m . After the adjustment of the algorithm itself, the error gradually decreased and finally became basically stable. In conclusion, SRCKF algorithm has the highest filtering accuracy and the best stability.

From Table 2, it can be seen that among the three algorithms, the estimation error range of carrier position based on SRCKF is the smallest, and the mean error in three directions is also much smaller than that of SRCDKF and SRUKF algorithms.

3.3. Additional experiments

In order to further reflect the superiority of SRCKF algorithm for position estimation of plant protection UAV, this paper also conducted several groups of experiments based on SRCDKF algorithm and SRCKF algorithm. The simulation conditions were consistent with the previous ones, and the simulation results were shown as follows:

It can be seen from the figure that the maximum estimation error based on SRCDKF algorithm is about 4m, and the maximum estimation error based on SRCKF algorithm is about 1.5m. In the first half of filtering, the former has a large error fluctuation, and the latter has faster convergence speed and better stability. In the second half of the simulation time, the filtering estimation errors of the two are basically in a small range, and the filtering is relatively stable.

It can be seen from the figure that there is little difference between the two algorithms in the estimation error in the y direction of the carrier position, which is related to the straight-line path and flight direction set by simulation. However, overall, the average error of the SRCKF based algorithm is slightly smaller than the average error of the SRCDKF algorithm, and its maximum error value is also lower than the latter. The error fluctuation is small, and the stability is good.

It can be seen from the figure that the estimation error range based on SRCDKF algorithm is $[-2.3, 2]$m, and the estimation error range based on SRCKF algorithm is [1,1] m . The latter has smaller average error and higher filtering accuracy.

From Table 3, it can be seen that the estimation error range of carrier position based on SRCKF is small, and its mean error is also much smaller than that of SRCDKF algorithm.

Table 2. Errors in three direction based on three algorithms

Parameters	SRCDKF	SRUKF	SRCKF
Mean error in the x-direction/m	1.0564	1.8922	−0.2135
Mean error in the y -direction/m	0.3581	−0.8940	0.1647
Mean error in the z-directio/m	1.2056	0.8063	0.2195
Simulation times	0.0246 s	0.0326 s	0.0129 s

Table 3. Error range in three direction based on two algorithms

Parameters	SRCDKF	SRCKF
Error range in the x− direction/m	$[-1.5, 4]$	$[-1.6, 1.2]$
Error range in the y− direction/m	$[-1.5, 3.8]$	$[-1, 2.1]$
Error range in the z− direction/m	$[-2.5, 2]$	$[-1.3, 0.9]$

4. Result discussions

This article is mainly based on the research of plant protection UAV structure design, navigation attitude control, and precise pesticide application technology. When implementing pharmaceutical spraying operations with UAVs, attention should also be paid to factors such as UAV nozzle leakage and the impact of pesticide deposition on crops, in order to determine the changes in crop growth environment parameters.

5. conclusions

In this paper, an attitude estimation algorithm of plant protection UAV based on SRCKF is proposed, and several groups of experiments are used to verify that SRUKF, SRCDKF and SRCKF are used to track and estimate the carrier position in x, y and z directions. The estimation errors of the three algorithms are compared, and it is known that the estimation error fluctuation range of the SRCKF algorithm is the smallest. The average error is the smallest, and the convergence speed is the fastest and the stability is the best.At the same time, the paper verifies that the filter estimation of the attitude Angle based on SRCKF algorithm can reduce the small roll angle error and pitch angle error of the carrier in a short time with a given azimuth error of $[0.8, 0.810]$. The algorithm can reduce the large course miscalibration angle error of the carrier to very small within the simulation 60s. Which ensured the precise positioning of the carrier pose and the precision of the navigation operation of the plant protection UAV, and improved the efficiency of precision agriculture.

This paper investigates the application of UAVs in plant protection, which have three main advantages:

1. It has the characteristics of low homework height, less drift, and can hover in the air. The downward airflow generated by the rotor during pesticide spraying helps to increase the penetration of logistics to crops, and has good control effects.

2. UAVs operate through ground remote control or GPS flight control, allowing spraying operators to operate remotely to avoid exposure to pesticides and improve the safety of spraying operations.

3. This paper provides simulation and verification of three methods for estimating the position information of UAVs, which provides certain reference value for the subsequent real flight environment of UAVs. The use of high-precision navigation can help improve the efficiency of precise pesticide application.

Funding

This research was funded by Henan Provincial Science and Technology Research Project, China(182102110295). Key Scientific Research Project of Colleges and Universities in Henan Province, China(21A590001). Key Scientific Research Project of Colleges and Universities in Anhui Province, China(2023AH051547, 2023AH051559). Key projects of Anyang Institute of technology's 2020 scientific research and Cultivation Fund, China(YPY2020001). The project of cultivating excellent young teachers of Anhui province, China(YQYB2023031). Teaching Quality Engineering Project of Anhui province, China(2023jyxm0796, 2023zygzts082). Teaching Quality Engineering Project of

Huainan Normal University, China(2023hskc06). Guiding scientific research projects in Huainan City(126).

Acknowledgments

Thank you for the funding from the Anhui Province Joint Construction Discipline Key Laboratory. Thank you for the support of Human-computer collaborative robot Joint Laboratory of Anhui Province. Especially the support of the aircraft simulation platform, which has provided basic support for the experiment in this paper.

Dandan Wang is a PhD candidate currently working at Huainan Normal University, with a main research focus on SINS and nonlinear filtering algorithms. Her five projects have received funding support from the provincial government, while her other projects have received funding support from other departments. She has published 10 SCI/EI papers and possesses rich teaching and strong research capabilities. .E-mail: lansejingling1988@126.com.

Zhaokun Zhu is a lecturer currently working at Zhengzhou Technology and Business University.His main research direction is electronic and communication engineering. In this article, he is mainly responsible for setting up the experimental environment. E-mail:512661241@qq.com. Kaituo Tan is a research assistant currently working at Huainan Normal University. His main research direction is automation technology. In this article, he is mainly responsible for experimental statistics and processing. .E-mail: lansejingling2015@126.com.

Hongjie Li is a lecturer currently working at Anyang Institute of Technology. His main research direction is electronic technology, and he usually helps the college handle some academic affairs. .E-mail:1871759023@qq.com.

Liang Yu is a lecturer currently working at Huainan Normal University, with a main research focus on mechanical design. One of his projects has received funding support from the provincial government and has been granted five patents. He has rich teaching experience. .E-mail:dandandejielun@163.com.

Conflicts of interrest

The funders had no role in the design of the study; in the collection, analyses, or interpretation of data; in the writing of the manuscript; or in the decision to publish the results.

References

[1] G. Hu, B. Gao, Y. Zhong, and C. Gu, (2020) *"Unscented kalman filter with process noise covariance estimation for vehicular ins/gps integration system"* **Information Fusion *64***: 194–204. DOI: https://doi.org/10.1016/j.inffus.2020.08.005.

[2] Y. Wang and Y. Li, (2021) *"Outlier detection based on weighted neighbourhood information network for mixed-valued datasets"* **Information Sciences *564***: 396–415. DOI: https://doi.org/10.1016/j.ins.2021.02.045.

[3] C. Henry, S. Poudel, S.-W. Lee, and H. Jeong, (2020) *"Automatic Detection System of Deteriorated PV Modules Using Drone with Thermal Camera"* **Applied Sciences *10***(11): DOI: 10.3390/app10113802.

[4] G. Hu, L. Xu, B. Gao, L. Chang, and Y. Zhong, (2023) *"Robust Unscented Kalman Filter-Based Decentralized Multisensor Information Fusion for INS/GNSS/CNS Integration in Hypersonic Vehicle Navigation"* **IEEE Transactions on Instrumentation and Measurement *72***: 1–11. DOI: 10.1109/TIM.2023.3281565.

[5] K.-C. Liao, H.-Y. Wu, and H.-T. Wen, (2022) *"Using Drones for Thermal Imaging Photography and Building 3D Images to Analyze the Defects of Solar Modules"* **Inventions *7***(3): DOI: 10.3390/inventions7030067.

[6] K.-C. Liao, J.-L. Liou, M. Hidayat, H.-T. Wen, and H.-Y. Wu, (2024) *"Detection and Analysis of Aircraft Composite Material Structures Using UAV"* **Inventions *9***(3): DOI: 10.3390/inventions9030047.

[7] P. Dong, J. Cheng, L. Liu, X. Sun, and S. Fan, (2019) *"A Heading Angle Estimation Approach for MEMS-INS/GNSS Integration Based on ZHVC and SAUKF"* **IEEE Access *7***: 154084–154095. DOI: 10.1109/ACCESS.2019.2948368.

[8] F. Andert, N. Ammann, S. Krause, S. Lorenz, D. Bratanov, and L. Mejias, (2017) *"Optical-aided aircraft navigation using decoupled visual SLAM with range sensor augmentation"* **Journal of Intelligent & Robotic Systems *88***: 547–565. DOI: 10.1007/s10846-016-0457-6.

[9] D. Gao, B. Hu, F. Qin, L. Chang, and X. Lyu, (2021) *"A Real-Time Gravity Compensation Method for INS Based on BPNN"* **IEEE Sensors Journal *21***(12): 13584–13593. DOI: 10.1109/JSEN.2021.3069960.

[10] S.-Y. Nabavi-Chashmi, D. Asadi, and K. Ahmadi, (2023) *"Image-based UAV position and velocity estimation using a monocular camera"* **Control Engineering Practice *134***: 105460. DOI: https://doi.org/10.1016/j.conengprac.2023.105460.

[11] A. Bakhshipour and A. Jafari, (2018) *"Evaluation of support vector machine and artificial neural networks in weed detection using shape features"* **Computers and Electronics in Agriculture *145***: 153–160. DOI: https://doi.org/10.1016/j.compag.2017.12.032.

[12] G. Popović, I. Cvišić, G. Écorchard, I. Marković, L. Přeučil, and I. Petrović, (2022) *"Human localization in robotized warehouses based on stereo odometry and ground-marker fusion"* **Robotics and Computer-Integrated Manufacturing *73***: 102241. DOI: https://doi.org/10.1016/j.rcim.2021.102241.

[13] D. Wang, K. Tan, Z.-H. Li, and G. Yuan, (2018) *"Research on Landmarks of SLAM Based on Square Root Cubature Kalman Filter"* **Journal of Physics: Conference Series *1069***:

[14] C. LI, J. MA, Y. YANG, B. XIAO, and Y. DENG, (2021) *"Adaptively robust multi-sensor fusion algorithm based on square-root cubature Kalman filter"* **Journal of Beijing University of Aeronautics and Astronautics *49***(1): 220–228(in Chinese). DOI: 0.1007/s11804-013-1164-y.

[15] L. Ye, Y. Yang, J. Ma, L. Deng, and H. Li, (2022) *"A Distributed Formation Joint Network Navigation and Positioning Algorithm"* **Mathematics *10***(10): DOI: 10.3390/math10101627.

[16] Y. Zhang, Y. Ding, J. Bu, and L. Guo, (2023) *"A Novel Adaptive Square Root UKF with Forgetting Factor for the Time-Variant Parameter Identification"* **Structural Control and Health Monitoring *2023***(1): 4160146. DOI: 10.1155/2023/4160146.

[17] D. Wang, K. Tan, Y. Q. Dong, G. Yuan, and X. Du, (2020) *"Estimating the position and orientation of a mobile robot using neural network framework based on combined square-root cubature Kalman filter and simultaneous localization and mapping"* **Advances in Production Engineering & Management**:

[18] J. Wang, J. Chen, L. Zhang, F. Xu, and L. Zhi, (2023) *"External force estimation for robot manipulator based on a LuGre-linear-hybrid friction model and an improved square root cubature Kalman filter"* **Industrial Robot**:

[19] L. Dang, W. Wang, and B. Chen, (2022) *"Square Root Unscented Kalman Filter With Modified Measurement for Dynamic State Estimation of Power Systems"* **IEEE Transactions on Instrumentation and Measurement *71***: 1–13. DOI: 10.1109/TIM.2022.3157005.

[20] X. Li et al., (2022) *"Research On Cooperative Control Technology And Application Of Wall-climbing Robot And UAV Based On Multi-sensing Fusion"* **Journal of Applied Science and Engineering *26***(5): 651–662.

[21] X. Jiang, Y. Deng, et al., (2021) *"UAV track planning of electric tower pole inspection based on improved artificial potential field method"* **Journal of Applied Science and Engineering *24***(2): 123–132.

[22] C.-T. Wu, C.-Y. Hsiao, C.-S. Chen, et al., (2013) *"An Assessment of Errors Using Unconventional Photogrammetric Measurement Technology-with UAV Photographic Images as an Example"* **Journal of Applied Science and Engineering *16***(2): 105–116.